Thermal Autofrettage of Dissimilar Material Brazed Joints

Niall Robert Hamilton, James Wood, David Easton, Mikael Brian Olsson Robbie, Yuxuan Zhang, Alexander Galloway

PII: S0261-3069(14)00940-6
DOI: http://dx.doi.org/10.1016/j.matdes.2014.11.019
Reference: JMAD 6970

To appear in: *Materials and Design*

Received Date: 20 May 2014
Accepted Date: 20 November 2014

Please cite this article as: Hamilton, N.R., Wood, J., Easton, D., Robbie, M.B.O., Zhang, Y., Galloway, A., Thermal Autofrettage of Dissimilar Material Brazed Joints, *Materials and Design* (2014), doi: http://dx.doi.org/10.1016/j.matdes.2014.11.019

Thermal Autofrettage of Dissimilar Material Brazed Joints

Niall Robert Hamilton[a], James Wood[a], David Easton[a] , Mikael Brian Olsson Robbie[a], Yuxuan Zhang[a], Alexander Galloway[a],

[a]University of Strathclyde, Department of Mechanical and Aerospace Engineering, Glasgow, United Kingdom, G1 1XJ

Corresponding author: James Wood, Tel: +44 (0) 141 548 2043, email:j.wood@strath.ac.uk, University of Strathclyde, Department of Mechanical and Aerospace Engineering, 75 Montrose Street, Glasgow, United Kingdom, G1 1XJ

Abstract

This paper presents a study on the effects of thermal autofrettage on the residual stresses in a Titanium – Copper brazed joint. It is shown that cryogenic thermal autofrettage has the potential to alter the residual stress field due to joining, in a manner that should result in an improvement in the subsequent operational fatigue performance of dissimilar material joints. Beneficial change in the residual stress field in the less-ductile component of the joint is apparent and desirable constitutive characteristics of the braze material to enhance the final residual stress field are also highlighted. Results from the finite element simulations are validated using experimental residual stress measurements produced using X-ray Diffraction. The characteristics of the process and the findings of the work presented should also be relevant to dissimilar material joints manufactured by other processes.

Keywords

Thermal autofrettage, residual stresses, finite element analysis, x-ray diffraction, validation.

1. Introduction

Residual stresses in dissimilar material joints have received significant attention in recent years and this is largely due to the damaging effects of these self-equilibrating stress fields on the fatigue and fracture behaviour of the joints. These studies cover a range of joining processes [1][2] including brazing [3][4][5]. Previous work has shown that finite element analysis (FEA) can be used to predict the residual stresses in a simple cylindrical Ti/72Ag-28Cu/Cu brazed joint and that due to relationships in parent material properties, the Ti develops a tensile axial and hoop residual stress along the free edge, with the Cu developing a compressive axial and hoop stress [6].

It has also been reported that in a similar fashion to the Ti/72Ag-28Cu/Cu joint, due to a similar relationship in material properties, for a range of brazed joints between a brittle material (W or ceramic) and a ductile material (stainless steel) the brittle material develops tensile axial and hoop residual stresses, while the ductile material develops compressive axial and hoop residual stresses [3][7]. The presence of large tensile residual stresses in a brittle material is generally undesirable and could reduce both the fatigue and ultimate strength of the joint. Due to the difference in material properties, stress relieving of these residual stresses is unlikely to be fully effective.

Thermal autofrettage has the potential to reduce the damaging tensile residual stresses that exist in a dissimilar material brazed joint due to the joining process. This involves cooling the joint after brazing to induce plastic work in the joint, caused by the differential thermal contraction of the materials, which in turn results in a reduction of the tensile residual stresses developed during joining. A detailed literature search has revealed that very little has been published in relation to the use of thermal autofrettage in general and as a post-joining process in particular.

In 2002, Barbero and Wen published details [8] of a “novel” thermal autofrettage process applied to composite metal-lined cryogenic pressure vessels, for which conventional mechanical autofrettage was not feasible. Kargarnovin, Zarei and Darijani used thermal autofrettage as a strengthening mechanism in a study of thick-walled spherical pressure vessels [9] in 2004. This study involved an elastic-perfectly plastic material model, did not involve dissimilar materials and relied on thermal gradients to induce plastic stresses. Darijani, Kargarnovin and Naghdabadi extended this work to linear strain hardening materials [10] in 2009.

The mechanism of thermal autofrettage is described in relation to the more common mechanical autofrettage process used to increase the durability of pressure vessels. Finite Element Analysis of the thermal autofrettage process has been conducted on both an idealised dissimilar material brazed joint without a brazed layer (a common but limited idealisation [11]) between an idealised ductile and brittle material and also in a dissimilar material joint with a brazed layer, namely a Ti/72Ag-28Cu/Cu joint. The effect of thermal autofrettage on the residual stresses in the Ti/72Ag-28Cu/Cu brazed joint is also examined using X-ray Diffraction (XRD) and comparisons made with the FEA predictions.

2. Thermal autofrettage of dissimilar material joints

In contrast to thermal autofrettage, mechanical autofrettage is a process that is commonly used to increase the load carrying capability and fatigue resistance of pressure vessels by internally pressurizing the structure beyond yield. This in turn induces beneficial compressive residual stresses

at the bore and enhances the yield stress in work hardening materials. The process of inducing compressive residual stresses by exceeding yield is highlighted in the following example of a beam in bending [12].

Yield occurs in the outer fibres of the beam when the applied moment M, equals the yield moment M_{yield}. If this moment is then increased to 1.5 x M_{yield} plastic strains develop through the thickness. (Note: an applied moment of 1.5 x M_{yield} corresponds to the limit load for a rectangular beam. In reality the autofrettage loads are generally far less than the limit load of the material). If this applied moment is then removed, local elastic unloading occurs parallel to the original elastic loading line as shown in Figure 1. The stress on the outer fibre does not return to zero when a moment of 1.5 x M_{yield} is removed, but instead a residual stress of -0.5 x σ_{yield} develops in the outer fibres. The graphs of applied moment and local stress on the extreme tensile fibre throughout this process are shown in Figure 1.

Due to the linear unloading, the stress distribution across section at limit load can be taken as the starting point to superimpose the unloading stresses to calculate the residual stress state as shown in Figure 2.

The effect of this self-equilibrating residual stress distribution is to extend the elastic range by 50% and induce beneficial compressive residual stresses on one surface of the beam, potentially influencing various failure mechanisms, including fatigue [11].

This principle of "over-loading" a structure to induce a beneficial compressive residual stress distribution can also be used to reduce the tensile residual stresses that can be found in dissimilar material joints due to the joining process. In this case the proposed loading is a cryogenic steady state temperature and the stresses arise from constraint on thermal contraction. This more unusual process of autofrettage can be achieved by cooling the brazed joint in a cryogenic freezer with either liquid nitrogen or helium. Figure 3 highlights the thermal autofrettage of a dissimilar material joint (neglecting the braze). In this example, an elastic material 2 (i.e. assumed not to yield for the purpose of this illustration) is being brazed to an elastic-perfectly plastic material 1. Material 1 is assumed to have a greater coefficient of thermal expansion than material 2 and a lower Young's modulus [11].

Initially, both materials are at a stress free state at the brazing temperature of 800°C (a). During cooling from the brazing temperature of 800°C to room temperature (b), the constraint of the interface due to the differential thermal expansion causes a compressive axial residual stress to develop in material 1, with a tensile residual stress developing in material 2. During cooling to room

temperature, plasticity develops in material 2 in close proximity to the interface. When an elastic–perfectly plastic material model is assumed for material 1, upon yielding the stiffness of material 1 reduces to zero hence no additional constraint can be applied to the joined material 2. This yielding effectively limits the stress in both materials.

After cooling to room temperature the sample is then slowly cooled in liquid nitrogen to -196°C (c). During this process, further plasticity develops in material 1 however no additional constraint is applied to material 2, in the areas of yield, due to the zero stiffness of material 1. Hence the stress in material 2, adjacent to the areas of yield in material 1, remains constant during this process. The joint is then heated back up to room temperature (d). During this stage both materials unload elastically causing a change in the stresses in both materials. For dissimilar material brazed joints such as those between a brittle material and a ductile material this will result in a reduction in tensile residual stresses in the brittle material adjacent to the joint.

A slow cooling rate avoids quenching the sample which could result in surface damage and large tensile residual stresses developing on the surface of the sample. Consequently the thermal autofrettage procedure developed for the experimental investigation in this section involves insulating the samples in low thermal conductivity polyethylene foam prior to storage in liquid nitrogen. The insulated samples are then wrapped in cling film to avoid the liquid nitrogen saturating the foam hence the only mode of heat transfer from the sample is due to conduction. One of the insulated samples prior to thermal autofrettage is shown in Figure 4:

3. FEA of thermal autofrettage of dissimilar material joints

3.1 FEA of thermal autofrettage of a dissimilar joint with braze layer included

Finite Element Analysis has been used to establish the effect of thermal autofrettage on a Ti/72Ag-28Cu/Cu joint. The Ti and Cu cylinders both have dimensions of 14mm in diameter and 25mm long, whilst the braze layer has a thickness of 80μm. The process and results will however be relevant to other combinations of materials, with similar dissimilarity in properties and joined by other processes. The simulation was performed using ANSYS 12.1, using two dimensional PLANE182 4-noded structural solid elements [13]. Two elements were used across the braze as a series of sensitivity studies [14] have shown that this is the minimum number of elements required to fully capture the constraint of the braze on the parent materials. The mesh, shown in Figure 5, was refined to an element size of 0.25mm at the interface and the model was held in the vertical direction by constraining the bottom surface to have zero vertical displacement. Axisymmetric conditions were assumed. Creep was not considered and the axisymmetric simplification assumes

perfect axial alignment of both materials. It has been shown that the residual stresses predicted by FEA are in reasonable agreement with those measured using XRD and that any transient effects due to differences in emissivity and thermal conductivity are negligible [6]. The FEA model used in previous work [6] to predict the residual stress distribution in the cylindrical Ti/72Ag-28Cu/Cu brazed joint was modified to include the thermal autofrettage process as shown schematically in Figure 5.

A previous transient thermal analysis of the thermal autofrettage process of the insulated sample starting at room temperature showed the sample would take c.1 hour to reach a uniform temperature of -196°C with a max cooling rate of -12°C/min. This cooling rate is based on the heat transfer coefficient between the polyethylene foam and liquid nitrogen being evaluated at a film temperature of -196°C. In terms of predicting the cooling rate this represents a worst case scenario as it neglects any air pockets in the cling film and over predicts the heat transfer coefficient. This maximum cooling rate of -12°C is considerably less than the initial cooling rate of the brazing process of c.-150C/min hence it was assumed that any transient effects during the thermal autofrettage process could be ignored. Consequently a simplified thermal stress analysis was used to model the thermal autofrettage process in a similar fashion to the simulation of the brazing process shown schematically in Figure 5.

If a small air gap of 1mm between the cling film and polyethylene foam is assumed and the heat transfer is evaluated at an average film temperature of -87.5°C the time taken to reach a uniform temperature of -196°C increases to c.8 hours. In reality the time required to reach -196°C will be less than this. Hence, to ensure that steady state thermal conditions were reached during the thermal autofrettage, the samples were stored in liquid nitrogen for c.8hours.

To model the thermal autofrettage in liquid nitrogen to -196°C the material properties of the Cu, Ti and 72Ag-28Cu were included in the model as shown in tables 1, 2 and 3. The properties of the Cu and Ti at -196°C were obtained from various literature sources [15][16] and the properties of the 72Ag-28Cu were linearly interpreted based on there being no phase changes within this temperature range. The properties of all materials at –196°C for use in FEA are summarised in Table 4.

The axial (z) residual stress distributions at the various stages of the thermal autofrettage process are shown in Figure 6. Upon cooling from the melting temperature of the 72Ag-28Cu (778°C) the residual stress field developed is as described in a previous study [6] (b). The change in axial stress due to cooling to -196°C (c) and then subsequent heating to back to 20°C (d) are also shown.

The FEA results in Figure 6 show a small decrease in the axial tensile residual stress field in the Ti due to the thermal autofrettage and a small decrease in the axial compressive residual stress in the Cu. The stress state developed during brazing and thermal autofrettage will be a function of the relationship in properties of all three materials in the joint [6]. However, it is postulated that the thermal autofrettage process has not been wholly successful, in this case, in causing a significant reduction in the initial residual stress state in the Ti due to significant strain hardening in the brazed layer (as shown in the engineering stress strain curve for the braze at room temperature and -196°C in Figure 7). The effectiveness of autofrettage in general is dependent on the development of plastic strains. Hence, it is further postulated that if the 72Ag-28Cu braze filler had both a lower yield stress and behaved in an elastic-perfectly plastic fashion, the thermal autofrettage process would be more effective in changing the initial residual stress distributions in both materials. This is examined in the following section. In addition to enhancing the effectiveness of the thermal autofrettage process, this change in material behaviour should also reduce the magnitude of the initial residual stress distribution due to brazing. There is also negligible change in the circumferential stress distributions in the strain hardening case.

3.2 FEA of thermal autofrettage of a dissimilar material brazed joint with an elastic perfectly plastic braze of lower yield stress

In this study the model set up and material properties for all three materials are identical to those used in the Ti/72Ag-28Cu/Cu joint discussed previously, the only difference being the yield stress and post yield stiffness of the braze filler. In this case a tangent modulus of 0.01GPa (not 0GPa to aid convergence) is used across all temperatures and the initial yield stress value for the braze in Table 1 and Table 4 have been halved. For this case the free edge axial distributions are shown during the thermal autofrettage process in Figure 8.

As shown, the initial axial residual stress (b) distribution with the elastic-perfectly plastic braze is similar to that with the 72Ag-28Cu braze however the magnitude of the residual stresses in both materials is less compared to the values shown in Figure 6. This is due to the reduced constraint applied by the elastic-perfectly plastic braze with a lower yield stress. Upon thermal autofrettage to -196°C, a slight increase in this residual stress distribution is seen due to a small increase in the yield stress of the braze, which applies an additional constraint to the Ti and the Cu.

Upon heating back up to room temperature (c) the thermal autofrettage process almost completely alleviates the axial residual stresses developed in the joint due to brazing (c. 100MPa stress relief in both materials in the region of the interface). This reduction is greater than the reduction seen in

Figure 6 which suggests an improvement in the autofrettage process due to the reduced yield stress and reduced strain hardening of the braze. In a similar fashion to the Ti/72Ag-28Cu/Cu dissimilar material joint there is a negligible difference in the circumferential stress distribution for this specific case. The concept of tailoring the properties of joining material to result in beneficial residual stresses is not new and Ooi et al [17] discuss the engineering of the phase transformation temperature of weld metal to provide improved residual stresses in welded joints. This has also been shown to improve the fatigue life for various geometries.

4. **Measurement of residual stresses after thermal autofrettage using XRD**

The change in residual stress due to the thermal autofrettage process has been measured using XRD on an axisymmetric Ti/72Ag-28Cu/Cu sample which was characterised after joining [6]. The results closest to the interface, at four angular locations 90° apart have been repeated after thermal autofrettage and compared to the original measured residual stresses and with those predicted by FEA.

The sample characterised was prepared as outlined previously. The XRD experimental set up, analysis parameters and uncertainty calculations are described in [6]. The parameters used for the XRD set up and evaluation of the residual stresses can be seen in Table 5 and a photo of the set up in Figure 9.

The measurements were obtained using a collimator of 1mm diameter with a maximum measurement depth of c.5μm [18] hence the residual stress readings are average values of stress in this irradiated volume. The shape and size of the irradiated area changes during the measurements and is a function of both 2θ and the value of Ψ tilt with a greater change in shape occurring at higher values of both of these parameters. For a 2θ angle of 60°, a Ψ tilt of 60° will result in an ellipse of approximately double the length of the original circular beam [19]. The sample is held in position at the correct height using a specially designed holder. For the measurements on the brazed sample, the distance from the braze is controlled correct to $\pm$0.01mm using a vernier caliper to move the sample within the holder however the initial alignment of the interface has been done by eye and is estimated to be correct to $\pm$ 0.5mm. For XRD readings on cylindrical samples the beam size has to be small in relation to the curvature of the specimen to reduce errors (maximum spot size of ¼ x sample radius)[10]. For samples 14mm diameter, this corresponds to maximum spot size of 7mm x 0.25 = 1.75mm, hence the beam size of 1mm can be assumed to be small in relation to the curvature of the sample.

There are three sources of uncertainty for the measurement due to; strain reading, assumed value of Young's modulus and repeatability of measurements [18]. Each residual stress measurement is accompanied by an x and y error bar based on uncertainty calculations. The error bars in the y-direction represent the combined uncertainty in the residual stress measurement with a 95% confidence level [6]. The error bars in the x-direction also give an indication of the surface area the results are averaged over. The original axial and circumferential XRD results and those measured after thermal autofrettage are shown in Figures 10 and 11 respectively along with the residual stress distributions predicted by FEA.

The measured axial residual stress in Figure 10 shows a reduction close to the interface at all four angular locations (0, 90, 270 degrees on specimen rotation). The average of the four angular locations closest to the interface is 57MPa, which reduces to an average of 4MPa after thermal autofrettage. FEA predicts a reduction of 30MPa at this location hence the small reduction in residual stress predicted by FEA is being reflected in the experimental sample. There are several possible reasons why the FEA over predicts the measured residual stresses. One is the simplified brazed layer material model is too stiff and the yield stress is too high. It is postulated that a better correlation could be obtained if a more accurate material model was used, which is not in fact easy to obtain for such a thin layer of material with a variation in structure and properties [20]. The second possible reason is that the assumption of a step change in material properties between the braze layer and the parent materials does not reflect reality and is over constraining the FEA model. The measured circumferential results, seen in Figure 11, show a smaller reduction in residual stress. The average circumferential stress closest to the interface prior to thermal autofrettage is 53MPa which reduces to 34MPa after thermal autofrettage; however there is one clear outlier in the test data (reading of 2MPa) and the reason for this is unknown. If this is neglected the average of the results after thermal autofrettage is 44MPa which improves the comparison.

These results show there is a reasonable correlation to the results predicted by FEA and those measured using XRD providing confidence that the thermal autofrettage process is having the desired effect in reducing the tensile stresses seen in the Ti, albeit with a small reduction for this Ti/72Ag-28Cu/Cu joint due to the near elastic behaviour of the filler. XRD results will under-predict the FEA stress magnitudes due to the fact that XRD is providing an average result over a 1mm spot size and depth of c. 5µm below the surface. In a rapidly changing stress field, these averaging effects can be significant.

6. Discussion

6.1 Practical issues of performing thermal autofrettage

The process of thermal autofrettage is limited by the temperature which the joint can be exposed to. The limit on this is absolute zero (-273°C) however this may not be practical in reality. For smaller components such as the Ti/72Ag-28Cu/Cu joints used in this work, storage in liquid nitrogen is straightforward if the component is sufficiently well insulated to prevent micro cracking due to thermal shock of the component. Cryogenic freezers which can cool to -80°C are commonplace and could be used to thermally autofrettage larger components - however the change in residual stress will be dependent on the reduction in temperature achieved. It is recommended that some form of NDT is used before and after thermal autofrettage to ensure the cooling process does not induce micro-cracking in the brazed interlayer. The sample reported herein was assessed for micro-cracking using dye penetrant testing and an optical assessment of the braze cross section after the residual stress measurements and no sign of micro-cracking was observed.

In addition to thermal autofrettage there also exists the opportunity to develop mechanical autofrettage for dissimilar material joints. This could be done by applying a compressive load perpendicular to the interface. Initial FEA of this case looked promising [14] and is the focus for further research.

Another practical consideration is the development of any further residual stresses during the thermal autofrettage procedure. The material model used for the braze filler at room temperature and at -196°C had a significant post yield stiffness which resulted in additional residual stresses being developed in the joint during the thermal autofrettage procedure. If this is the case, care needs to be taken to ensure that this does not cause failure in the joint during the thermal autofrettage process. There also exists the possibility that some materials will have a ductile to brittle transition in the thermal autofrettage temperature range which could affect both simulation and experimental results for the residual stresses [17][21].

In addition, a dissimilar material joint in a real structure is likely to be between components of more complex geometry and this would have to be taken into account in the development of a viable and useful thermal autofrettage procedure.

6.2 Possible Further Developments

Further FEA and XRD validation of the thermal autofrettage process is currently being conducted on other combinations of materials and brazing fillers. Ideally one of the fillers used in future should behave close to elastic-perfectly plastic which should result in more significant changes in the residual stress field.

In addition, the effects of thermal autofrettage should be correlated directly to an improvement in either joint strength or mechanical and thermal fatigue performance and hence future experimental validation of the process should include a series of specimens and tests to facilitate this.

6.3 Effect of residual stresses on failure mechanisms

The combination of stresses developed in the joint due to joining and subsequent operational loads will govern the performance of the joint in operation. The relevance of the residual stresses due to joining on any failure mechanism will be dependent on whether the parent materials present in the joint are brittle or ductile in nature and whether failure occurs in the parent materials or at the interface. The significance of these residual stresses on various failure mechanisms is briefly discussed and whether thermal autofrettage is likely to affect the failure mechanism.

Tensile residual stresses will influence failure in brittle materials and at the interface. Tensile residual stresses could cause the joint to fail during manufacturing or combine with operation loads to cause failure in service. As shown, thermal autofrettage could be used to reduce damaging tensile residual stresses found in dissimilar material joints due to joining, however care must be taken to ensure the thermal autofrettage process itself does not cause failure of the joint. While this did not happen in this investigation, it is clearly a possibility.

Plastic collapse only occurs under a primary load, with ductile materials. Residual stresses in dissimilar material joints are self-equilibrating and are unlikely to influence plastic collapse, hence it is unlikely that altering the initial residual stress field using thermal autofrettage will influence the plastic collapse load of a joint between dissimilar ductile materials. However it is possible that residual stresses could influence other failure mechanisms which in turn lead to plastic collapse. Ratcheting in ductile materials is dependent on initial plastic straining and subsequent accumulation, which will be influenced by residual stresses. Buckling instability is a function of the stress state existing in a body and could be affected by the initial residual stress distribution at joints.

Tensile residual stresses due to joining are generally detrimental to fatigue life. Conversely compressive residual stresses in the surface layers are usually beneficial and can improve fatigue life. Fatigue failure could occur in either the parent materials or the interface between the braze and the parent materials. Thermal autofrettage could be used to influence the initial residual stress field to improve the fatigue performance of the joint.

7. **Conclusions**

The process of thermal autofrettage has been presented as a method of altering the residual stress field due to joining in dissimilar material brazed joints and in doing so reducing the potentially damaging tensile residual stresses that may be present after the joining process. By modifying residual stresses, the overall stress state can be altered beneficially when combined with operational stresses. Finite Element Analysis of the change in residual stress in a Ti/72Ag-28Cu/Cu dissimilar material brazed joint due to thermal autofrettage is in reasonable agreement with the change measured using XRD. It is postulated that due to the stress – strain response of the 72Ag-28Cu filler, the change in residual stress due to thermal autofrettage is beneficial but relatively small. Studies have shown however that if the braze filler has both a lower yield stress and tends towards behaving in an elastic-perfectly plastic fashion, the thermal autofrettage process can be more effective in reducing the tensile residual stresses due to joining. In addition, the initial residual stresses developed in the joint will be less, due to the reduced constraint on both materials. This could result in the thermal autofrettage process being used to improve the performance of dissimilar material joints which are susceptible to brittle failure and fatigue.

The thermal autofrettage process is not limited to dissimilar material brazed joints and should be relevant for other methods of joining such as diffusion bonding, HIPing, electron beam welding and explosion welding. Possibilities may also exist in the areas of deposition technologies such as laser and weld cladding.

The main conclusions drawn from this study are as follows:

- Thermal autofrettage can be used as a means of altering the residual stress field due to joining and to reduce the tensile residual stresses that are present after the joining process. This could result in an improvement in the operational performance of dissimilar material joints.
- It has been demonstrated that thermal autofrettage could significantly change the initial residual stress distribution due to joining, depending on the plastic properties of the braze filler.
- The work presented in this paper is not only relevant to dissimilar material brazed joints but also dissimilar material joints manufactured by other processes.
- Care must be taken during the thermal autofrettage process so as not to damage the joint, through micro-cracking or otherwise.

Acknowledgement

This work was completed with support from the Culham Centre for Fusion Energy [22].

References

[1] Ramana PV, Reddy GM, Mohandas T, Gupta AVSSKS. Microstructure and residual stress distribution of similar and dissimilar electron beam welds- maraging steel to medium alloy medium carbon steel. Mater Des 2010;31:749–60.

[2] Jiakun Liu, Jian Cao, Xiaoguo Song, Yifeng Wang, Jicai Feng. Evaluation on diffusion bonded joints of TiAl alloy to Ti3SiC2 ceramic with and without Ni interlayer: Interfacial microstructure and mechanical properties. Mater Des 2014;57:592–597.

[3] B. Kalin, V. Fedotov, O. Sevrjukov, A. Moeslang, and M. Rohde, "Development of rapidly quenched brazing foils to join tungsten alloys with ferritic steel," Journal of Nuclear Materials, vol. 329–333, pp. 1544–1548, Aug. 2004.

[4] G. Blugan, J. Kuebler, V. Bissig, and J. Janczak-Rusch, "Brazing of silicon nitride ceramic composite to steel using SiC-particle-reinforced active brazing alloy," Ceramics International, vol. 33, no. 6, pp. 1033–1039, Aug. 2007.

[5] M. I. Seki, T. I. Horie, T. Tone, K. Nagata, K. Kitamura, M. Shibui, T. Araki, and Y. Shibutani, "Fatigue strength of tungsten - copper for divertor plates duplex structures," Journal of Nuclear Materials, vol. 155–157, pp. 392–397, 1988.

[6] N. Hamilton "Thesis - The development of residual stresses in, and thermal autofrettage of, dissimilar material brazed joints" University of Strathclyde - Department of Mechanical and Aerospace Engineering, 2013.

[7] P. Bastid and P. Jackson, "Predicting successful manufacture of ceramic/metal joints using Weibull modelling," TWI Report 852/2006, 2006.

[8] E.J. Barbero and E.W. Wen, "Autofrettage to Offset CTE Mismatch in Metal-Lined Composite Pipes," Composite Materials: Testing and Design Fourteenth Volume, ASTM STP 1436, C.E. Bakis, Ed., ASTM International, 2002.

[9] M.H. Kargarnovin, A.R. Zarei and H. Darijani, "Wall thickness optimisation of thick-walled spherical vessel using thermo-elasto-plastic concept," International Journal of Pressure Vessels and Piping, v82, pp379-385, 2005.

[10] H. Darijani, M.H. Kargarnovin and R. Naghdabadi, "Design of spherical vessels under steady-state thermal loading using thermo-elaso-plastic concept," International Journal of Pressure Vessels and Piping, v86, Issues 2-3, Feb-Mar 2009, pp143-152.

[11] N. Hamilton, J. Wood "The metallurgy, mechanics, modelling and assessment of dissimilar material brazed joints " Journal of Nuclear Materials, pp 42-51, 2012.

[12] E.J. Hearn, Mechanics of Materials 2 – An introduction to the mechanics of elastic and plastic deformation of solids and structural materials. Butterworth Heinemann, 3rd Ed., p73-75, 1999.

[13] "Ansys Element Reference." Ansys Inc., Release 12.1, pp1189-1196, November 2009.

[14] T. Peat, "An investigation into the modelling of dissimilar material joints and the application of autofrettage to reduce residual stresses," University of Strathclyde - Department of Mechanical and Aerospace Engineering - Masters Project Thesis, 2012.

[15] "Material Property Database (MPDB)." JAHM Software, 2012.

[16] ASM Handbook Volume 2: Properties and Selection: Nonferrous alloys and special-purpose materials. 1990.

[17] S.W. Ooi, J.E. Garnham, T.I. Ramjaun, "Review: Low transformation temperature weld filler for tensile residual stress reduction," Mater Des 2014;56:773–781.

[18] M. Fitzpatrick, A. Fry, P. Holdway, F. Kandil, J. Shackleton, and L. Souminen, "Determination of residual stresses by X-ray diffraction - Issue 2," Measurement Good Practice Guide, v52, 2005.

[19] U. Kocks, Texture and Anisotropy - Preferred orientations in polycrystals and their effect on material properties. Cambridge University Press, p144, 1998.

[20] Y, Zhang, A. Galloway, J. Wood, M.B.O. Robbie, D. Easton, "Interfacial metallurgy study of brazed joints between tungsten and fusion related materials for divertor design," J. Nucl. Mater. v454, pp207-216, Nov. 2014.

[21] G.M. Schnier, J. Wood, A. Galloway, "Investigating the Effects of Process Variables on the Residual Stresses of Weld and Laser Cladding," Advanced Materials Research. v996, pp481-487, 2014.

[22] http://www.ccfe.ac.uk/, (Accessed: 20th October 2014).

Figure 1 Moment and stress on outer fibre of elastically perfectly plastic beam in bending with an applied moment of 1.5 x M_{yield}

Figure 2 Stress distribution across a beam in bending with applied moment of 1.5 x M_{yield}

Figure 3 Thermal autofrettage of a dissimilar material brazed joint

Figure 4 Insulated sample for thermal autofrettage to -196°C in liquid nitrogen

Figure 5 Thermal Autofrettage of Ti/72Ag-28Cu/Cu dissimilar material brazed joint and associated finite element model

Figure 6 Axial stress distribution during thermal autofrettage cycle of Ti/72Ag-28Cu/Cu brazed joint

Figure 7 Engineering stress strain curves at -196°C and 20°C
(see Tables 1-3 for moduli and yield stresses)

Temp (°C)	k (W/mK)	C_p (J/KgK)	α x 10^{-6} (/K)	E (GPa)	σ_{yield} (MPa)	E_{tan} (GPa)
20	493	291	15.3	59.2	170	30
100	495	306	19.7	59.2	146.7	26.1
200	472	313	21.1	59.2	117.5	21.2
300	460	323	21.3	49.8	88.3	16.3
400	459	339	21.3	31.6	59.2	11.4
500	440	342	21.4	17.2	30	6.5
600	420	350	20.1	11	19.2	4.2
700	413	362	17.8	7.8	8.4	1.8
778	404	369	16	0	0	0

Table 1 Summary of 72Ag-28Cu material properties for use in FEA

Temp (°C)	k (W/mK)	C_p (J/KgK)	α x 10^{-6} (/K)	E (GPa)	σ_{yield} (MPa)	E_{tan} (GPa)
20	386	383	16.7	125	40	0.1 x E
100	385	393	17	121	32.4	0.1 x E
200	383	403	17.5	115	24.3	0.1 x E
300	380	413	17.8	109	17.6	0.1 x E
400	375	421	18.2	103	12.4	0.1 x E
500	368	429	18.6	96	8.9	0.1 x E
600	360	437	19	90	6.6	0.1 x E
700	354	446	19.3	83	5.9	0.1 x E
778	348	455	19.6	77	6.4	0.1 x E

Table 2 Summary of CuC110 material properties for use in FEA

Temp (°C)	k (W/mK)	C_p (J/KgK)	α x 10^{-6} (/K)	E (GPa)	σ_{yield} (MPa)	E_{tan} (GPa)
20	21	524	8.5	109	356	0.1 x E
100	20	542	8.8	105	246	0.1 x E
200	19	566	9	99	160	0.1 x E
300	18	589	9.1	93	111	0.1 x E
400	19	611	9.2	87	83	0.1 x E
500	19	630	9.4	81	66	0.1 x E
600	20	645	9.6	75	57	0.1 x E
700	21	666	9.8	69	53	0.1 x E
778	21	736	10	65	51	0.1 x E

Table 3 Summary of Ti grade 2 material properties for use in FEA

Material	α x 10^{-6} (/K)	E (GPa)	σ_{yield} (MPa)	E_{tan} (GPa)
Ti	6.5	123	556	0.1 x E
Cu	14	136	66	0.1 x E
72Ag-28Cu	15.3	59.2	220	40

Table 4 Material properties for thermal autofrettage at -196°C

XRD parameters	Ti	Cu
System	Bruker D8 Advance	Bruker D8 Advance
Radiation source	Cu Kα	Cu Kα
Diffraction plane	Ti 2 1 3	Cu 4 2 0
2θ	139°	137°
Tube voltage	40kV	40kV
Tube current	40mA	40mA
Collimator diameter	1mm	1mm
Method	Omega tilt, iso-inclination, sin2ψ	Omega tilt, iso-inclination, sin2ψ
ψ tilt values	+ 0°, 5°, 10°, 15°, 20°, 25°, 30°, 35°, 40°,45°,50°	+ 0°, 9°, 18°, 27°,36°, 45°
Φ values	0°, 45°, 90°	0°, 45°, 90°
Stress model	Biaxial + shear	Biaxial + shear
Peak evaluation	Pearson VII	Pearson VII

Table 5 Summary of residual stress measurement parameters

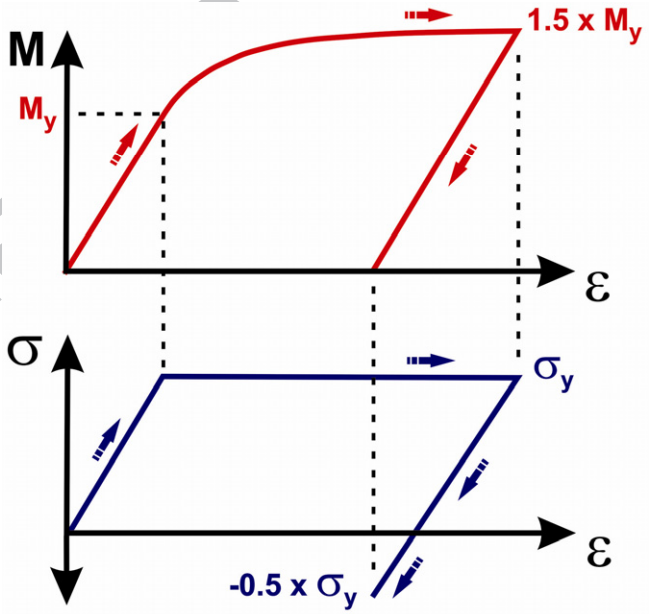

Figure 1 Moment and stress on outer fibre of elastically perfectly plastic beam in bending with an applied moment of 1.5 x M_{yield}

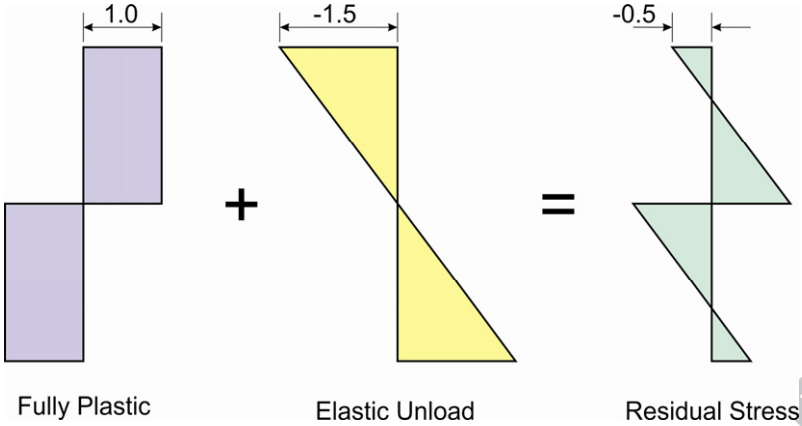

Figure 2 Stress distribution across a beam in bending with applied moment of 1.5 x M_{yield}

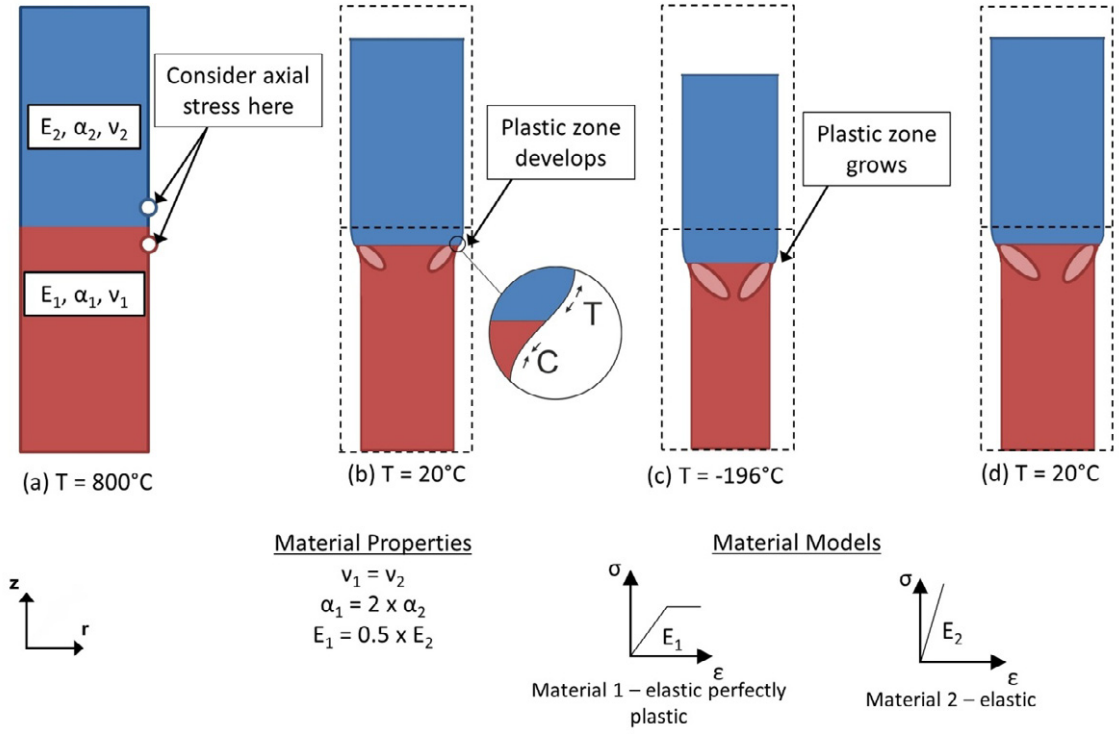

Figure 3 Thermal autofrettage of a dissimilar material brazed joint

Figure 4 Insulated sample for thermal autofrettage to -196°C in liquid nitrogen

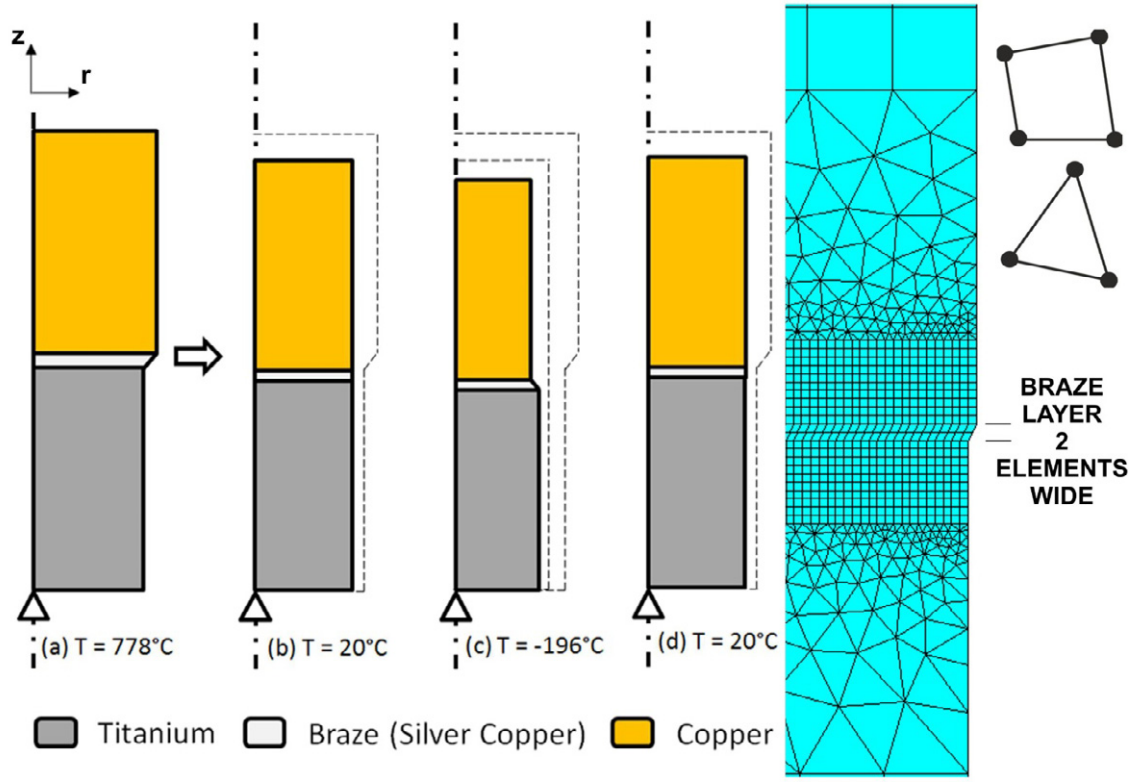

Figure 5 Thermal Autofrettage of Ti/72Ag-28Cu/Cu dissimilar material brazed joint and associated finite element model

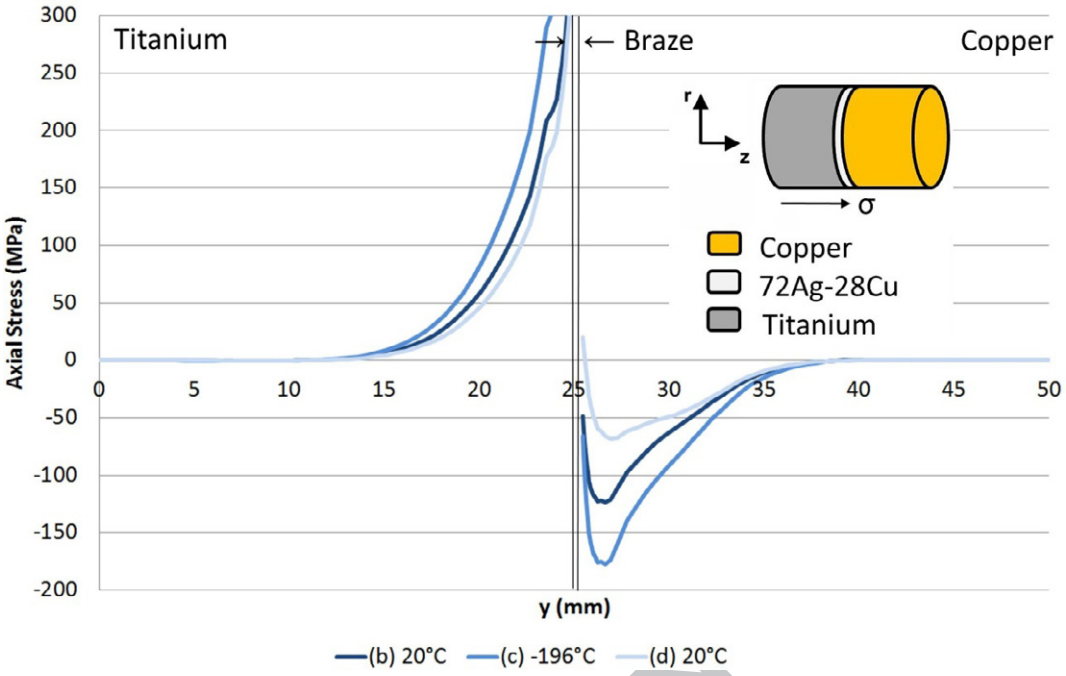

Figure 6 Axial stress distribution during thermal autofrettage cycle of Ti/72Ag-28Cu/Cu brazed joint

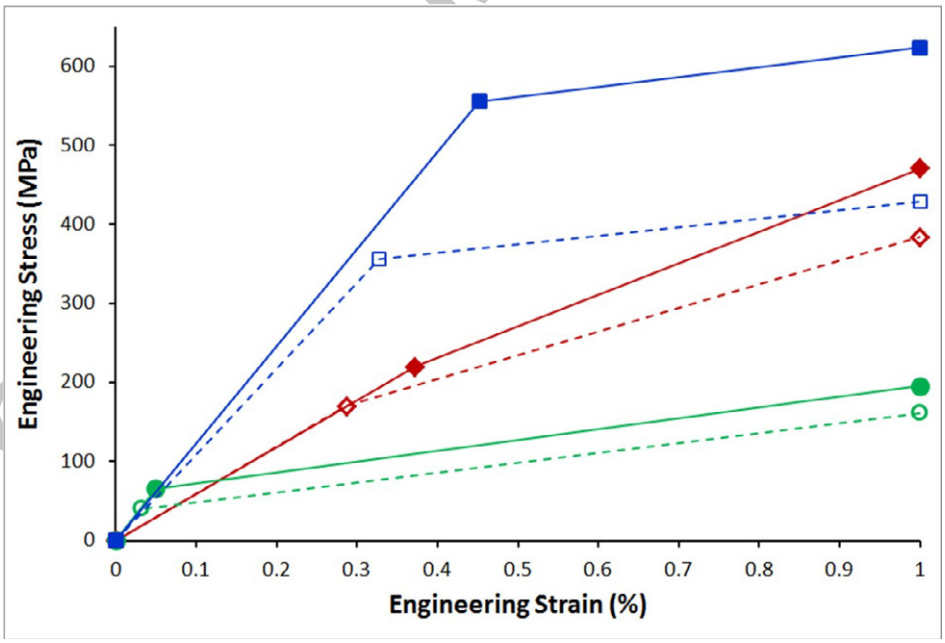

Figure 7 Engineering stress strain curves at -196°C and 20°C
(see Tables 1-3 for moduli and yield stresses)

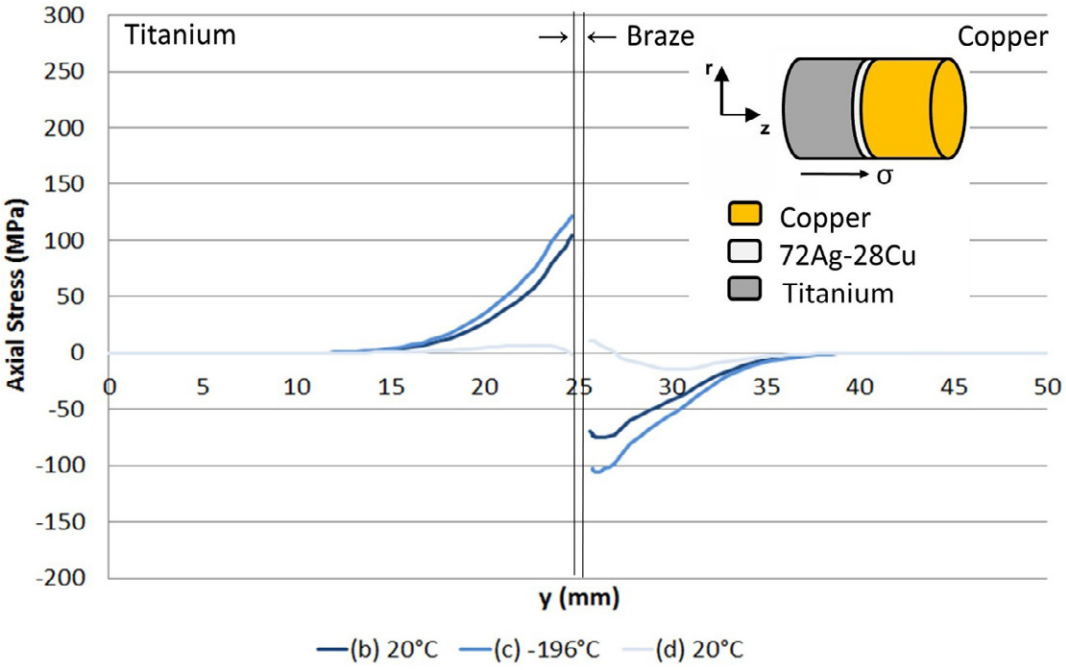

Figure 8 Axial stress distributions of a Ti – Cu brazed joint with an elastic perfectly plastic braze

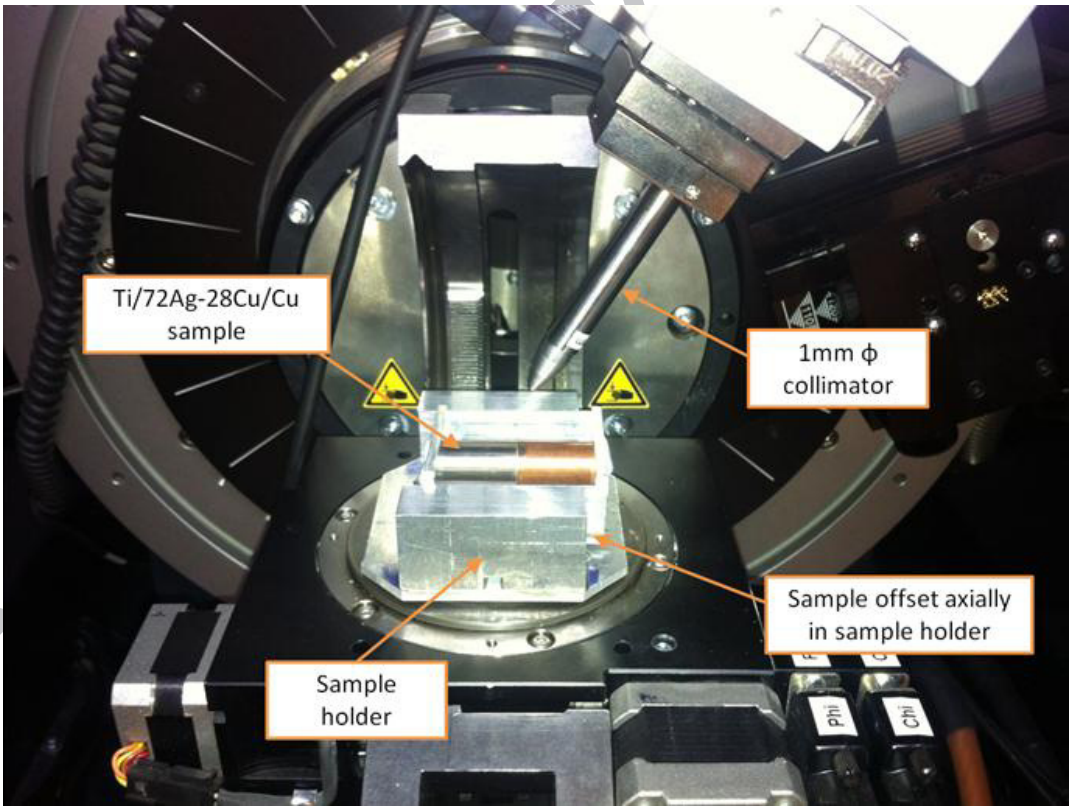

Figure 9 XRD Set up

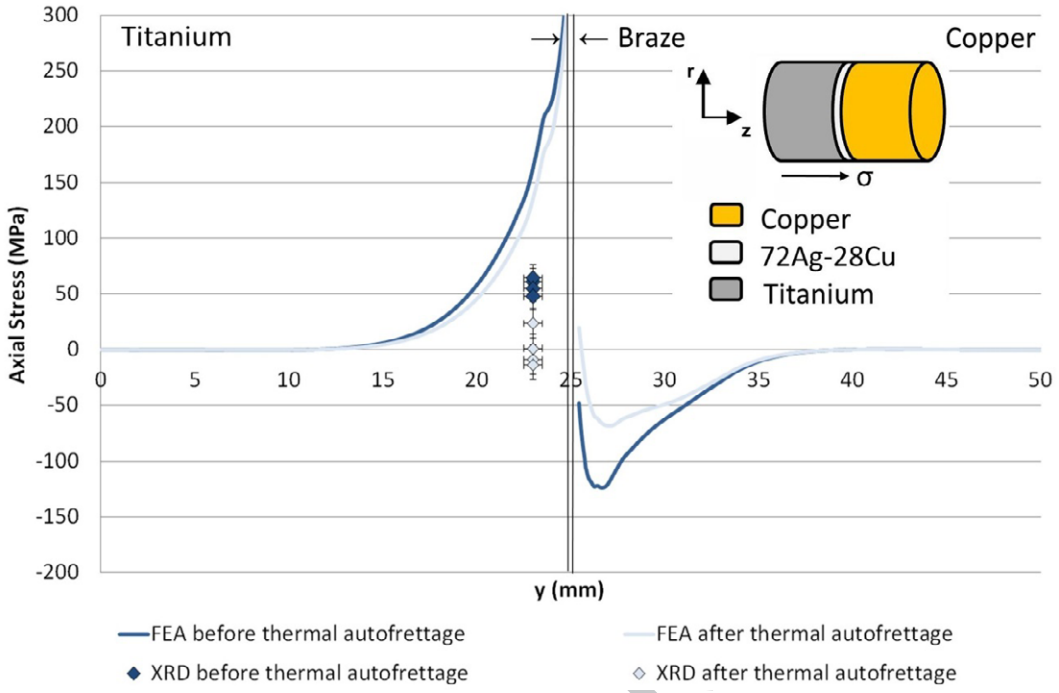

Figure 10 Measured axial residual stress before and after thermal autofrettage

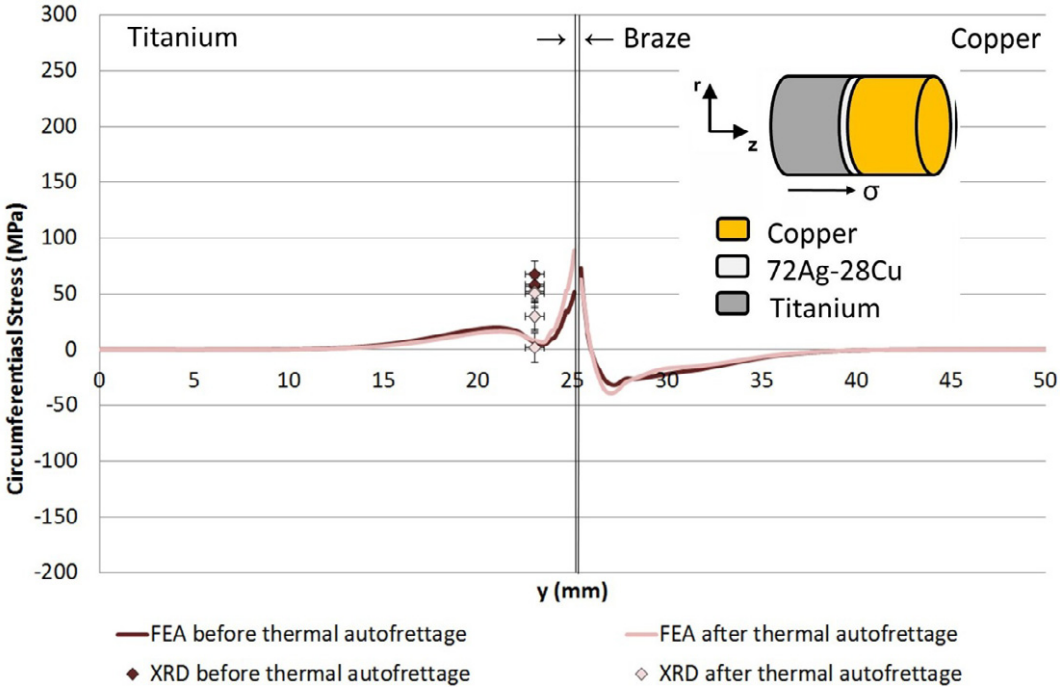

Figure 11 Measured circumferential residual stress before and after thermal autofrettage

- The beneficial effects of cryogenic thermal autofrettage on residual stresses in a dissimilar joint is shown.
- Desirable constitutive material characteristics are highlighted.
- FE simulations are validated with experimental residual stress measurements using X-ray diffraction.